Università di Pisa

Facoltà di Medicina e Chirurgia Scuola di Specializzazione in Radiodiagnostica

Direttore: Prof. Davide Caramella

Tesi di Specializzazione

Monitoring of thermal-induced changes in liver stiffness during controlled hyperthermia and microwave ablation in an ex-vivo bovine model with point shear wave elastography

Relatore:

Chiar.mo Prof. Davide Caramella

Candidata:

Dott.ssa Giulia Gherarducci

Anno Accademico 2015/2016

SUMMARY

ABSTRACT

Purpose

In point shear wave elastography (pSWE), an acoustic radiation force impulse (ARFI) is used to generate shear-waves in liver tissue. Shear wave velocity (SWV) reflects the underlying tissue stiffness, which varies during the heating process. In order to investigate how liver stiffness changes during heating, we designed this two phases study. The first phase was conducted in controlled hyperthermia and aimed to (1) quantify the temperature dependence of liver tissue stiffness as measured with SWV (2) identify the threshold value of SWV related to coagulation (3) assess the reproducibility of this measurement and (4) evaluate the irreversibility of stiffness changes. The second phase was conducted during microwave (MW) ablation to (1) confirm the SWV threshold for the stiffness of coagulated tissue during MW ablation and (2) determine the reliability of pSWE to delineate the boundaries of ablation zone.

Materials and Methods

In phase 1 of the study 5 cuboidal samples of ex-vivo bovine liver were uniformly heated to target temperatures ranging 40-100°C and then cooled down until 50°C. B-mode ultrasound (US) imaging and pSWE were acquired simultaneously (Virtual Touch^{TM} Tissue Quantification, Siemens Healthcare) and SWV, expressed in m/s, was measured in a fixed region of interest (ROI, < 1cm^2) at set temperatures (2.5-5°C

intervals). Tissue temperature was recorded by two thermocouples positioned at 1.5 cm from the ROI. The threshold value of SWV at 60°C (avg60), the temperature for immediate tissue coagulation, was identified. In phase 2, 11 samples were ablated by a commercial MW ablation system (HS AMICA®, H.S. Hospital Service SpA). B-mode US imaging and SWV were acquired simultaneously. MW ablation was performed at 60 W until avg60 + 0.5 m/sec was reached in a ROI that was placed 1.5 cm radially from the antenna feed point. Afterwards, SWV was measured in several ROIs at established distances ranging from 10 mm to 40 mm from the antenna feed, acquiring 10 SWVs for each ROI. Finally, the specimens were cut along the antenna to obtain gross-pathology of the coagulation necrosis. A SWV contour map was created, superimposing the pathology picture of the liver necrosis with the B-mode US images of ROIs' positions. To each point at pathology the following values were assigned: 0=outside, 0.5= at the border, and 1=within necrosis. The correlation of mean values of SWV with location at gross-pathology was evaluated.

Results

In phase 1 experiments a steep transition in liver stiffness was observed at 63.0 ± 2.4°C with an average SWV value of 3.54 ± 0.68 m/s (baseline value: 1.41 ± 0.17 m/s at room temperature). A decrease in SWV was observed up to 42°C (-0.31 ± 0.07 m/s with respect to baseline), a gradual increase was detected up to 55-60°C, and the described transition followed above 60°C. Avg60, defined as mean SWV at 60°C, was of 2.5 m/sec. This pattern was observed in all experiments, with very similar

SWV/temperature curves. The changes in liver stiffness proved to be irreversible, as average SWV values of 4.40 ± 0.41 m/s were measured in the cool-down cycles. In phase 2, in 8 of the experiments, interrupted when SWV of 3 m/s was measured in the studied ROI, the ROI was at the inner side of the necrotic area border at pathology (accuracy 89%). SWV values measured in ROI valued at pathology as outside (0), border (0.5), and within (1) necrosis were dispersed. No correlation between SWV values for outside (0), border (0.5), and within (1) necrosis could be identified.

Conclusion

SWV is useful to monitor thermal changes in tissue in the setting of controlled hyperthermia. pSWE can provide a velocity threshold predictive of the presence of coagulation necrosis during MW ablation in ex-vivo liver model. The complexity of ablation process in tissues, and possibly the shrinkage occurring after ablation, makes pSWE not able to reliably capture changes of stiffness within, at the border, and outside the necrotic zone in this experimental model.

INTRODUCTION

Non-invasive monitoring of percutaneous thermal ablation is essential for preventing complications while ensuring treatment efficacy. While ultrasound (US) or computed tomography (CT) are generally used for guiding the insertion of applicators into the tumours, magnetic resonance (MR) imaging is currently the only modality with validated techniques for real-time temperature monitoring [1, 2].

Elastography is a non-invasive US- or MR-based technique that is able to assess the mechanical properties of tissues. During heating an increase of tissue stiffness is observed, that is quantitatively measurable [3]. Tissue elasticity changes after coagulation have been measured using various elastography techniques including either US-based methods, such as transient elastography (TE) and acoustic radiation force impulse (ARFI) techniques, or MR elastography [4]. Although MR generally provides excellent contrast between tumour and normal tissue and can be used to monitor thermal ablation therapies, this modality is expensive and not easily incorporated into real-time guidance [5]. So that, US-based elastography methods have drawn increasing interest in the evaluation of tissue stiffness of tumours during thermal ablation [6]. Many US-based thermal ablation monitoring techniques are under investigation; however, among those techniques, ARFI methods are unique that can provide quantitative estimation and mapping of tissue stiffness in real-time [7]. Using ARFI technique - that propagates shear waves and generates localized,

displacements in tissue - shear wave velocity (SWV) is measured in m/s choosing the exact location (region of interest, ROI) of measurements under B-mode US visualization [8].

A search through the Literature suggests that relationship between tissue stiffness and heating temperatures can be further investigated, to describe in detail thermal effects on liver tissue mechanical properties. It is well known that during thermal ablation, coagulation, which involves protein denaturation and tissue dehydration, occurs almost instantaneously at temperatures above 60°C, whereas water vaporization, the main source of artefacts in B-mode US, occurs above 100°C [3].

To investigate how heating produces changes in liver stiffness, a homogenously heated sample of ex-vivo bovine liver tissue was used in the first phase of the experiments, to reduce causes of variability in the measurements and precisely investigate the relationship between temperature and stiffness changes as quantified by SWV. We then moved in the second phase to a sample of liver tissue that was heated with a microwave (MW) antenna, to reproduce in the laboratory a situation that was similar to clinical practice. The first phase of the study was aimed to (1) quantify the temperature dependence of liver tissue stiffness as measured with SWV (2) identify the threshold value of SWV related to coagulation (3) assess the reproducibility of this measurement and (4) evaluate the irreversibility of stiffness changes. The second phase was aimed to (1) confirm the SWV threshold for the

stiffness of coagulated tissue during MW ablation and (2) determine the reliability of pSWE to delineate the boundaries of ablation zone.

MATERIALS AND METHODS

Study design

The study was organised in two phases, the first conducted in conditions of controlled hyperthermia, heating homogenously an ex-vivo liver sample; the second during MW ablation (Fig.1). In the first and second phase, five and eleven experiments were performed respectively.

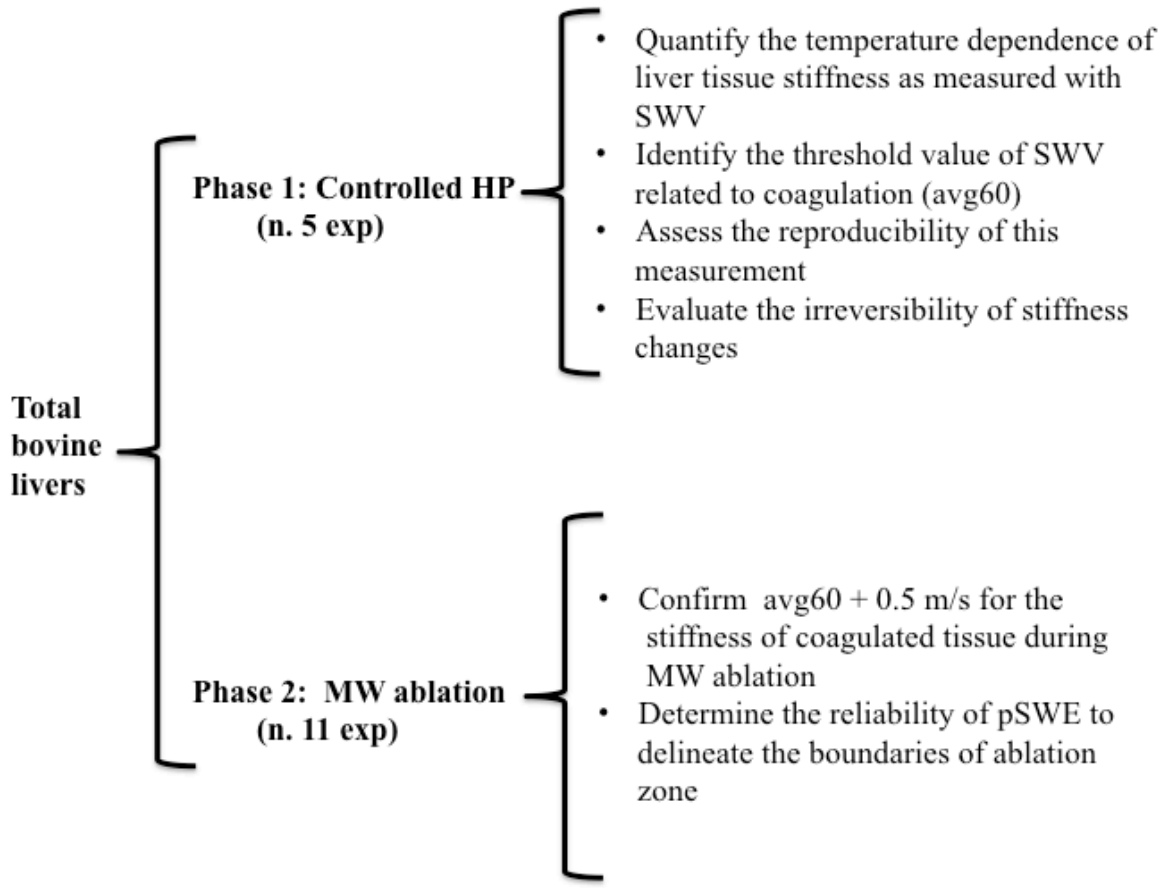

Fig 1. Study design and aims

Experimental set-up

Phase 1

Five various-sized cubes (dimensions ranged between 60×40×20 mm^3 and 80×90×50 mm^3) of ex-vivo bovine liver were cut from larger blocks of tissue (up to 6 kg) chosen for their high degree of uniformity, avoiding major vessels whenever possible. A bipolar RF system with two aluminium clamp electrodes was used to uniformly heat the samples to target temperatures. The aluminium clamps were attached on the

sample and connected to the RF generator (HS Amica GEN H 1.0) via a coaxial cable (Fig. 2A). The generator can supply a power up to 200 W at 450 kHz. Additionally, two thermocouples (19 G x 150 mm) were inserted parallel in the centre of the sample, spaced approximately 30 mm from each other, to monitor the heating temperatures. (Fig.2B)

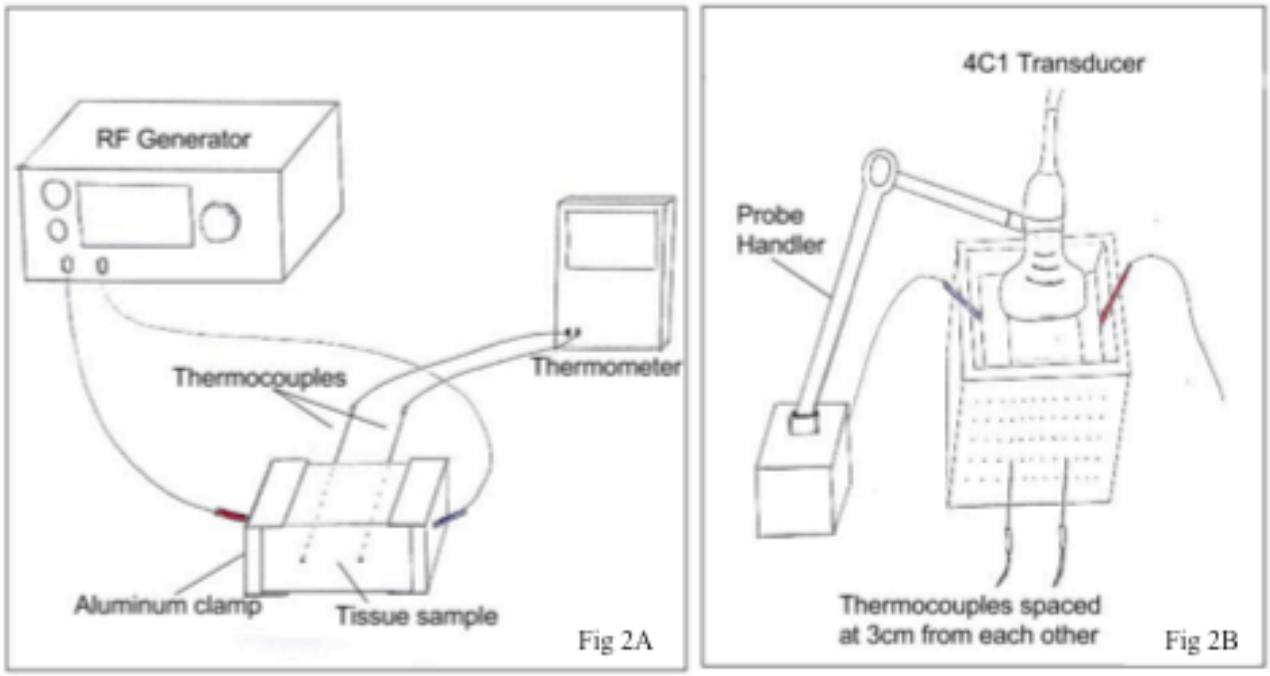

Fig 2. Scheme of experimental set-up. (A) Two aluminium clamps were attached on the sample and connected to the RF Generator that was used to heat the samples. (B) Liver specimens were encased in a multi-perforated box where the two thermocouples were inserted at a distance of 30 mm apart. The probe was then fixed above the box.

ARFI elastography was performed with a Siemens Acuson S2000™ US system (Siemens Healthcare, Erlagen, Germany) with a 4C1 transducer, by using Virtual Touch™ Tissue Quantification application. The SWV was exhibited in m/s and if the

amount of non-shear wave motion exceeded a threshold of 4.99 m/s, the system displayed a non-numerical result (X.XX) on the screen (Fig. 3). For computational needs, to calculate mean and standard deviation, we decided to consider this non-numerical value as 5 m/sec.

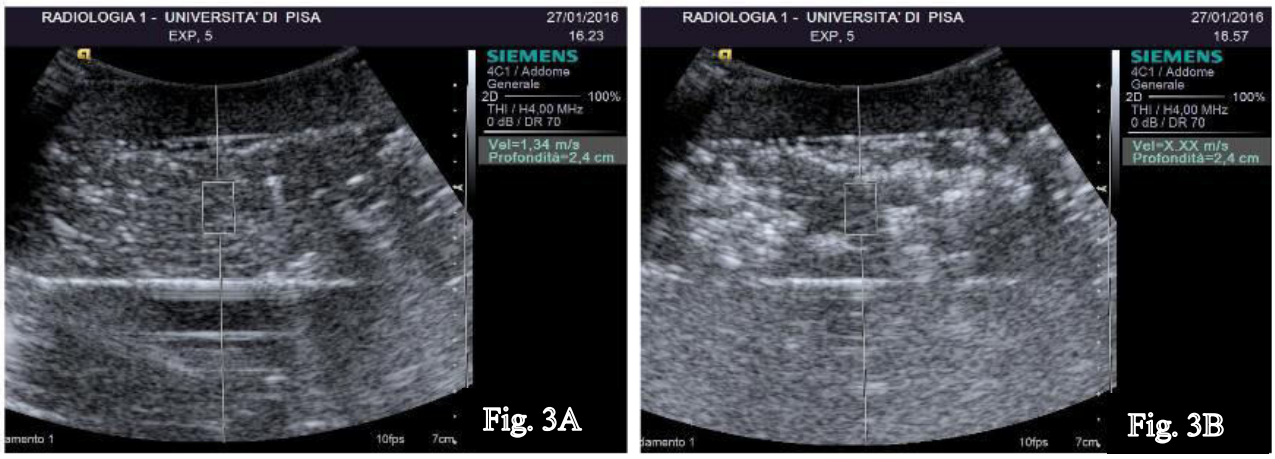

Fig 3. B-mode images showing a pre-ablation **(A)** and post-ablation **(B)** SWV measured in a fixed small ROI of the same liver tissue specimen.

The contact between the transducer and the surface of the sample was ensured by Ultrasound gel pad (Aquaflex, 2x9 cm, Parker Laboratory Inc.) (Fig. 4A). To avoid any displacement during the procedure, the specimens were encased in a box of 100x100x140 mm^3 with two opposite surfaces containing rows and columns of multiple holes spaced at 0.5 cm intervals in order to let thermocouples access in the liver tissues samples. The transducer was then fixed with a probe handler above the tissue. (Fig. 4)

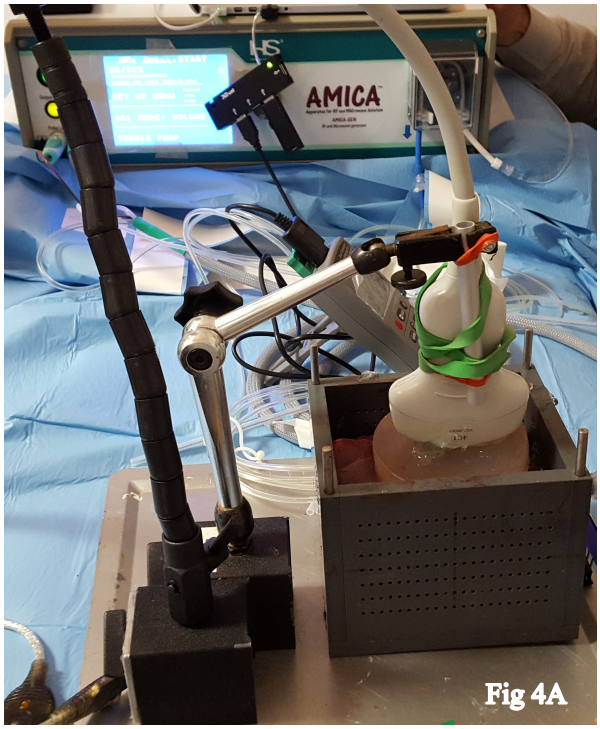

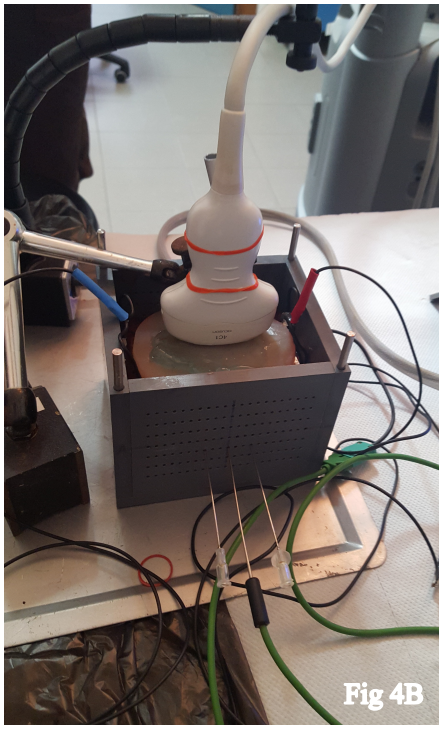

Fig 4. Experimental set-up. The surface between the specimens and the probe was ensured by an aqueous gelatine matrix **(A)** and thermocouples access into the box from the multi-perforated surface **(B)**.

Before each experiment, temperature of tissues was measured to ensure an initial pre-ablation temperature within the range of 18–24°C. In addition, an initial liver SWV value > 2 m/s was an exclusion criterion because such high value before any treatment revealed an artefact due to liver compression by the probe. When compression for technical reasons occurred, SWV measures cannot be considered reliable and we chose to readjust the probe and retake the measures.

Liver samples were then heated to target temperatures between 40 and 100°C: 5°C intervals between 40°C and 55°C, 1°C interval from 55 to 70°C and then 10°C intervals until 100°C was reached. In the course of the heating phase, power of 40W was applied until the target temperature was obtained; power was then reduced and

controlled manually in order to keep the tissue temperature constant (± 0.9°C variability around target temperature). At each target temperature, 11 consecutive readings of SWV were obtained from a small ROI of 8 mm long and 5 mm wide. The temperature of the first appearance of X.XX m/sec and the number of non-numerical measurements at a specific target temperature were recorded.

Knowing that immediate coagulation occurs in liver tissue above 60°C, avg60, defined as mean value of SWV at 60°C, was calculated.

The mean SWV and their respective standard deviations at each target temperatures were calculated. Temperature/SWV curves were then generated and visually compared to investigate experiments' reproducibility.

After the heating at 100°C, samples were submitted to cool-down cycles and readings were obtained every 10°C until the thermocouples showed a temperature of 50°C. Mean SWV was calculated and the temperature at which all measurements were non-numerical was recorded.

Phase 2

Eleven various-sized cubes (dimensions ranged between 80×70×60 mm^3 and 80×90×50 mm^3) of ex-vivo bovine liver were cut from larger blocks of tissue (up to 6 kg). To prevent any displacement during the procedure, the specimens were encased in a box of 100x100x140 cm, as described before. An Ultrasound gel pad ensured the contact between the transducer and the surface of the sample (Aquaflex, 2x9 cm, Parker Laboratory Inc.). The ablation system used was a commercial MW ablation

system (HS AMICA®, H.S. Hospital Service SpA); the antenna was placed in the centre of the sample, in parallel with the probe. (Fig. 5)

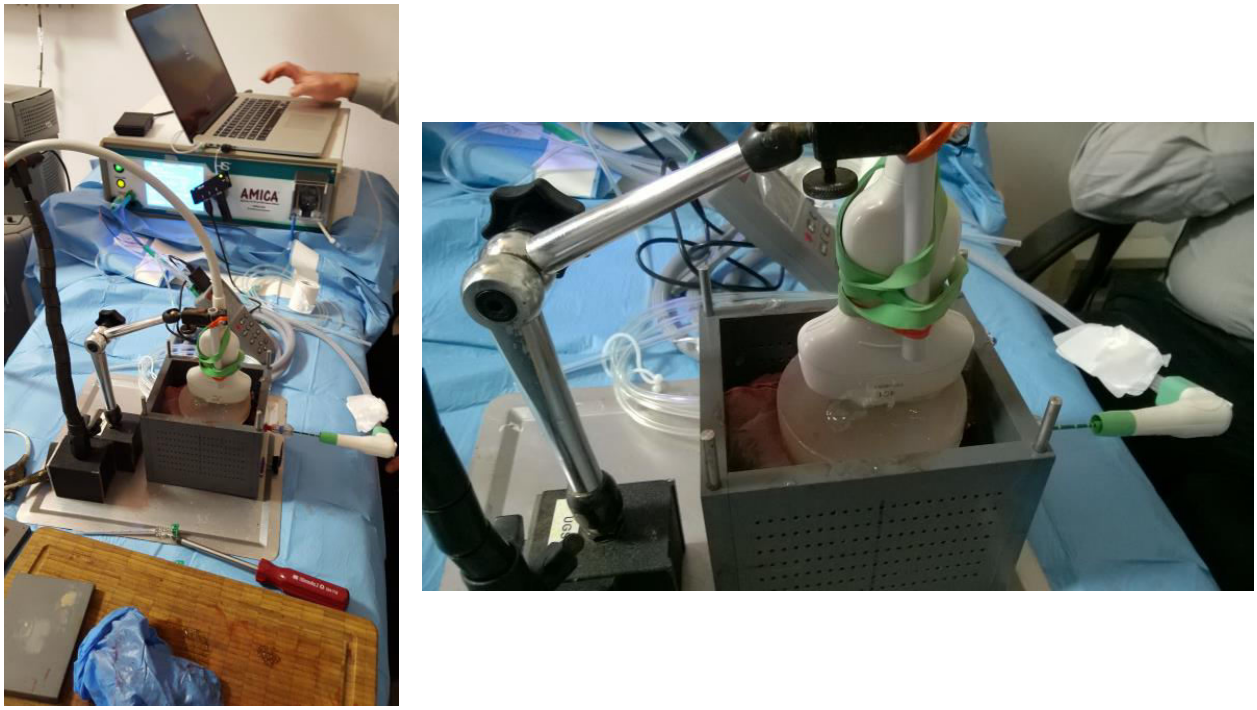

Fig 5. Photographs illustrating data acquisition setup: the transducer was oriented in parallel with the antenna and fixed with a probe-handler in contact with the gel pad. The ablation system used was a commercial MWA system (HS AMICA®, H.S. Hospital Service SpA) with a 14G antenna.

Liver stiffness was measured before each experiment. The value > 2 m/s was an exclusion criterion revealing an artefact due to liver compression by the probe. When compression for technical reasons occurred, SWV measures cannot be considered reliable and we chose to reposition the probe and retake a measure.

Liver samples were then heated with MW ablation that was performed at 60 W, until avg60 +0.5 m/sec was reached in a ROI <1 cm^2 that was placed 1.5 cm radially

from the antenna feed point. (Fig. 6)

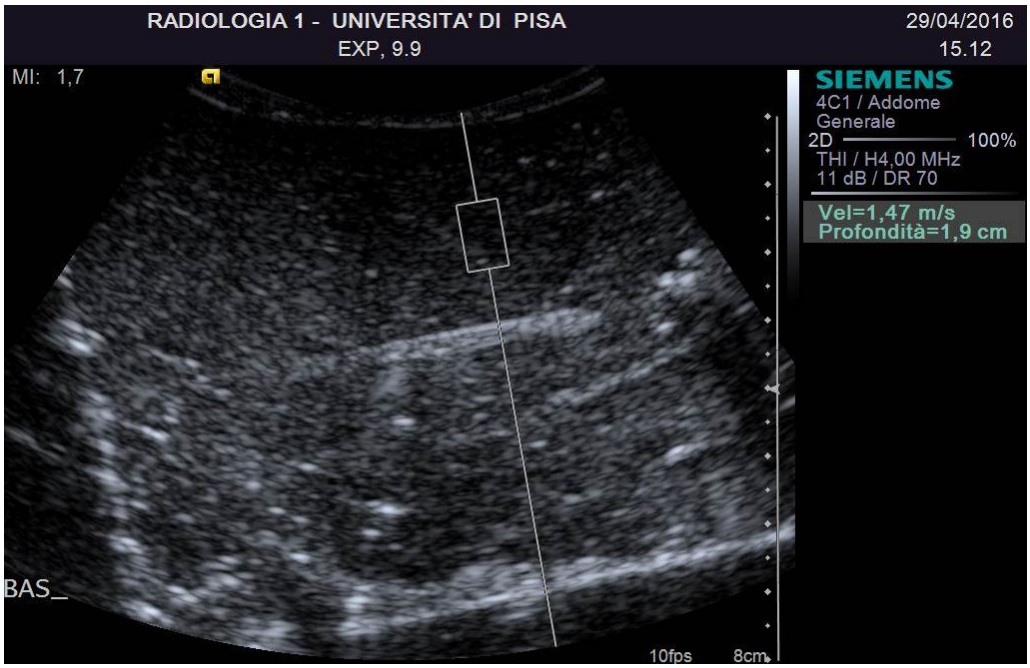

Fig 6. Showing baseline measurement in the ROI that was placed 1.5 cm radially from the antenna feed point.

Afterwards MW ablation was stopped and SWV was measured in several ROIs at established distances ranging from 10 mm to 40 mm from the antenna feed, acquiring 10 SWV determinations for each ROIs. Cartesian coordinate system was used to place the ROIs on the US image. The antenna tip was assumed as the origin, the antenna profile and the line perpendicular to it were considered the XY axes. ROIs were placed at 1 cm distances in this Cartesian system (Fig.7A,B). The same Cartesian coordinate system was superimposed to pathological specimen and used to correlate pathology with the SWV measured in ROIs. (Fig. 7C)

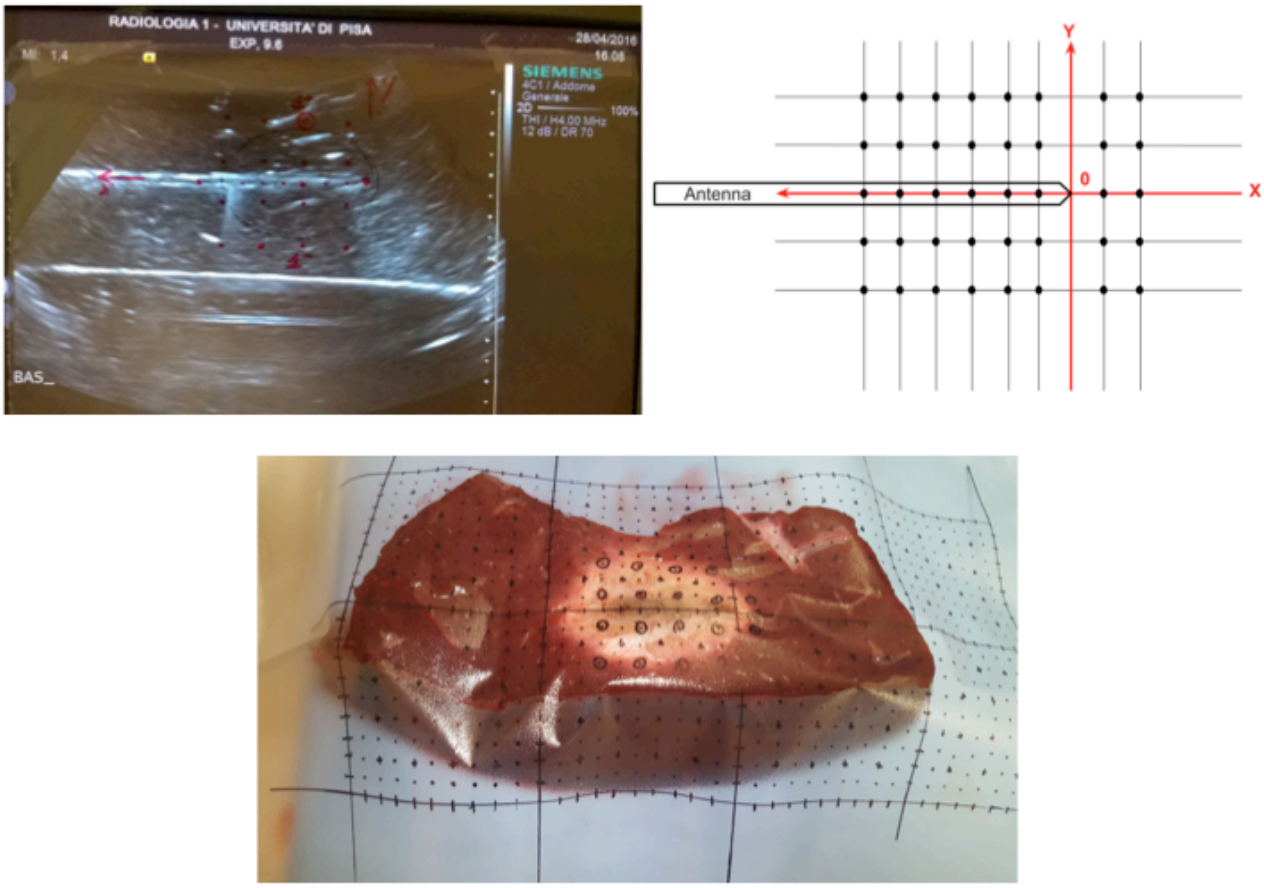

Fig. 7 Image showing the superimposed Cartesian coordinate system used to place the ROIs in the US image **(A)**. The antenna tip was assumed as the origin, the antenna profile and the line perpendicular to it were considered the XY axes. ROIs were placed at 1 cm distances in this Cartesian system **(B)**. The same Cartesian coordinate system was superimposed to pathological specimen and used to correlate pathology with the SWV measured in ROIs **(C)** .

To each point at pathology the following values were assigned: 0=outside ablation area; 0.5=border; 1=within necrosis. For those points evaluation of the mean SWV values was performed.

point Shear Wave Elastography (pSWE)

pSWE imaging is a non-invasive technique that is implemented in an US system and is able to assess the mechanical properties of tissues. It involves the use of ARFI technology that generates shear waves, which propagate into the tissue. Shear waves are generated in the liver in a small ROI and B-mode imaging is used to monitor the displacement of liver tissue. From the displacements monitored over time at different locations from the ARFI pulse, the SWV is calculated in meters per second (m/s). (Fig. 8). Assumptions can then be made that can convert the SWV in meters per second to the Young modulus in kilopascals: $E = 3 (vS^2 \cdot r)$, where E is the Young modulus, vS is the SWV and r is the density of the tissue in homogeneous isotropic tissues. In reverse, TE shear wave velocity measurements are typically expressed as the Young modulus in kilopascals [4]. pSWE differs from the first-generation TE in several aspects, including the generation of shear waves within the organ by a focused ultrasound beam and the capability of focusing the beam at different locations within the organ under ultrasound image guidance [9].

pSWE was performed with a Siemens Acuson S2000™ ultrasound system (Siemens Healthcare, Erlagen, Germany) with a 4C1 transducer, by using Virtual Touch™ Tissue Quantification application. ·

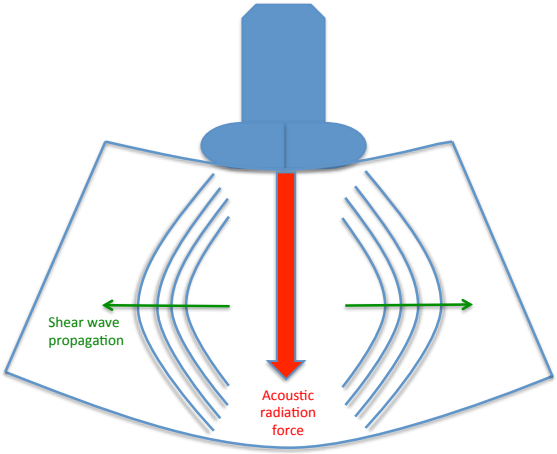

Fig. 8 ARFI imaging: an initial US pulse in transmitted at diagnostic intensity level (baseline signal) and used for later comparison. Then a short duration (0.3 s) high-intensity acoustic pulse is transmitted and followed by a series of diagnostic intensity pulses, used to track the displacement of the tissue caused by the pushing pulse.

RESULTS

Phase 1

Outcomes of the experiments, conducted on the five cubes of ex-vivo liver tissue as a function of temperature, are presented in Table 1.

Description	Symbol	Meas Unit	Avg	Std Dev	Max	Min	Semi-D	xp1	xp2	xp3	xp4	xp5
SWV_avg @ baseline	V_{BL}	m/s	1,41	0,17	1,67	1,24	0,22	1,452	1,383	1,240	1,670	1,290
Transition temperature, i.e. lowest temperature yielding at least 1 occurrence of X.XX out of 11 consecutive SWV samples	T_{TR}	°C	62,97	2,40	65,15	58,90	3,13	63,100	58,900	63,575	64,100	65,150
N° of X.XX occurrences out of 11 consecutive SWV samples @ transition	N_{TR}	-	4,00	2,74	8,00	1,00	3,50	5	1	8	4	2
SWV_avg @ transition	V_{TR}	m/s	3,54	0,68	4,35	2,75	0,80	3,826	2,911	4,350	3,870	2,750
SWV increase over baseline @ transition (V_{TR} - V_{BL})	$\Delta_{V,TR}$	m/s	2,13	0,68	3,11	1,46	0,83	2,374	1,528	3,110	2,200	1,460
SWV_StdDev @ transition	$\sigma_{V,TR}$	m/s	1,03	0,18	1,13	0,71	0,21	1,091	0,710	1,120	1,100	1,130
SWV_avg @ 60°C	V_{60}	m/s	2,50	0,52	3,20	2,03	0,59	3,200	2,900	2,030	2,090	2,280
T[°C]_ @ SWV>2.5 m/s	$T_{2.5}$	°C	60,40	2,30	62,00	57,00	2,50	57,000	59,000	62,000	62,000	62,000
Minimum SWV detected	V_{min}	m/s	1,10	0,15	1,31	0,97	0,17	1,189	0,967	0,969	1,308	1,043
Temperature @ V_{min}	T_{min}	°C	41,98	2,46	46,25	40,00	3,13	40,000	41,600	41,250	40,775	46,250
V_{BL} - V_{min}	$\Delta_{V,min}$	m/s	0,31	0,07	0,42	0,25	0,08	0,263	0,416	0,271	0,362	0,247
SWV decrease rate until 40°C	ΔV/ΔT	m/sK	-0,0180	0,0054	-0,0132	-0,0274	0,0071	-0,027	-0,016	-0,017	-0,016	-0,013
SWV_avg @ post-heating	V_{POST}	m/s	4,4042	0,4059	4,9360	3,8730	0,5315	4,173	4,436	4,603	3,873	4,936
SWV_StdDev @ post-heating	$\sigma_{V,post}$	m/s	1,0520	0,4683	1,7750	0,4770	0,6490	0,936	1,107	0,965	1,775	0,477

Tab. 1 shows the results obtained from the experiments (xp1-5) with SWV-related expressed in m/s.

The mean baseline SWV of the five specimens, before heating, was 1.41 ± 0.17 m/s at room temperature. The heating of bovine liver tissue induced a linear decrease of SWV up to 42°C (-0.31 ± 0.07 m/s with respect to baseline) with a minimum average SWV detected (1.10 m/s) at this temperature. Then SWV gradually increased up to 55-60°C corresponding to an average SWV value of 2.50 ± 0.52 m/s. At a

temperature threshold of 63°C ± 2.4°C, that we called “transition temperature”, we observed a steep increase in SWV. At this temperature, at least 1 out of 11 consecutive measurements and a maximum of 8 non-numerical measurements (X.XX) occurred as a result of a dramatic change of SWV. The mean SWV at this temperature was 3.54 ± 0.68 m/s. In two out of five sessions (xp4 and xp5) we reached a temperature above 63°C (respectively 64°C and 65°C); in these cases the gross pathology photographs confirmed the presence in the specimens of large vessels.

Avg60, i.e. the mean SWV at 60°C, was 2.5 m/s. To be conservative we decided to use, as threshold for coagulation in the Phase 2 of the study, the threshold of avg60 + 0.5 m/sec, i.e. 3 m/sec.

Repeated experiments revealed a reproducible pattern of tissue mechanical changes during heating in ex-vivo bovine liver, with very similar, overlapping temperature/SWV curves (Fig. 9). Only the first (xp1, in blue line) SWV/temperature curve presented a slightly different shape, probably due to the insufficient familiarity with the set-up.

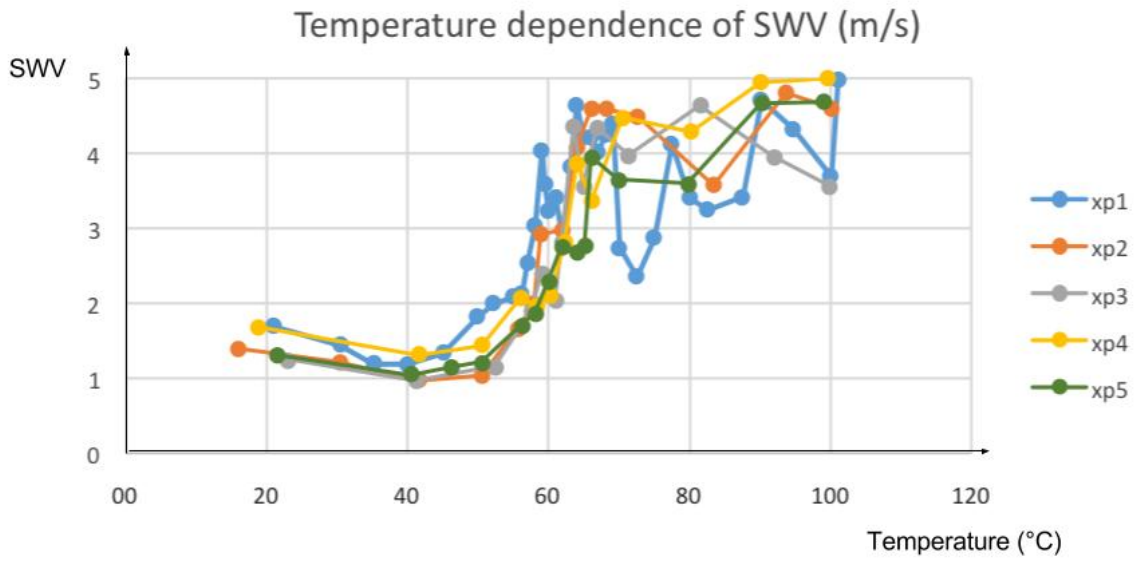

Fig. 9. Curves SWV/temperature in different experiments. In all the

In the cool down we measured SWV values of 4.40 ± 0.41 m/s at post-heating temperatures, every 10°C from 100°C until 50°C was reached. At around 50°C of each experiment, the 11 measurement showed X.XX, proving the irreversibility of changes in liver stiffness.

Phase 2

In 3 cases the experiment results were not considered reliable due to thecnical problems occured during the procedure. In 8 experiments, interrupted when SWV of 3 m/s was measured in the established ROI, the ROI was at the inner side of the border of the ablated tissue, in necrotic area. The accuracy in determining the presence of necrosis was therefore of 89%. (Fig. 10)

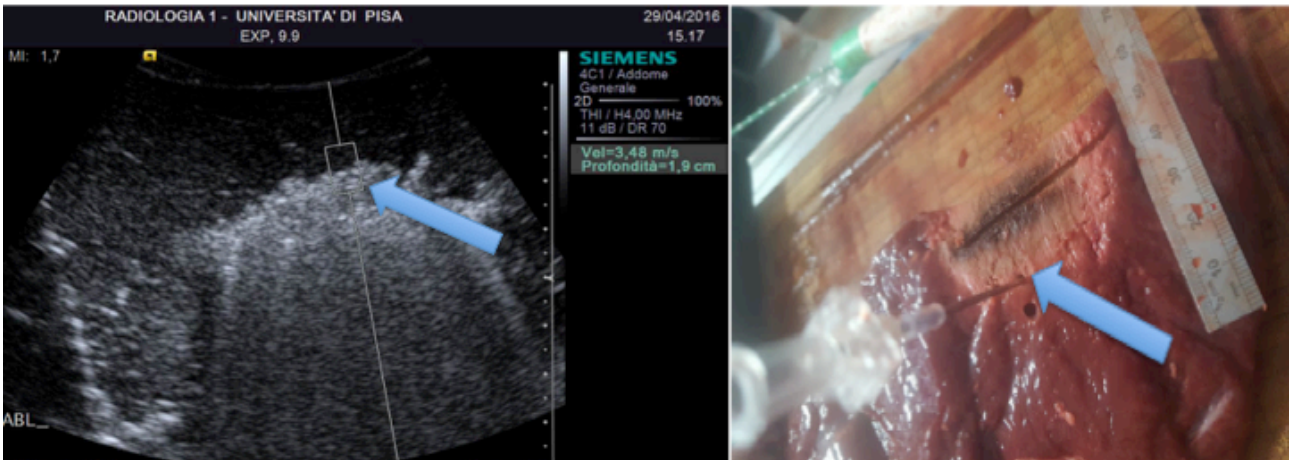

Fig 10. The ablation was interrupted when 3 m/sec were measured in the ROI at 1.5 cm from the antenna feed (A). The same region was demonstrated to be in the inner side of the border of the ablated tissue, in necrotic area (B).

In the post-ablation analysis we graphically correlated the SWV values and the gross pathology, classifying points as outside (0), border (0.5), and within (1) the ablated area. SWV values measured in ROI valued at pathology as outside (0), border (0.5), and within (1) were dispersed. No SWV threshold values for outside (0), border (0.5), and within (1) could be identified. (Fig.11)

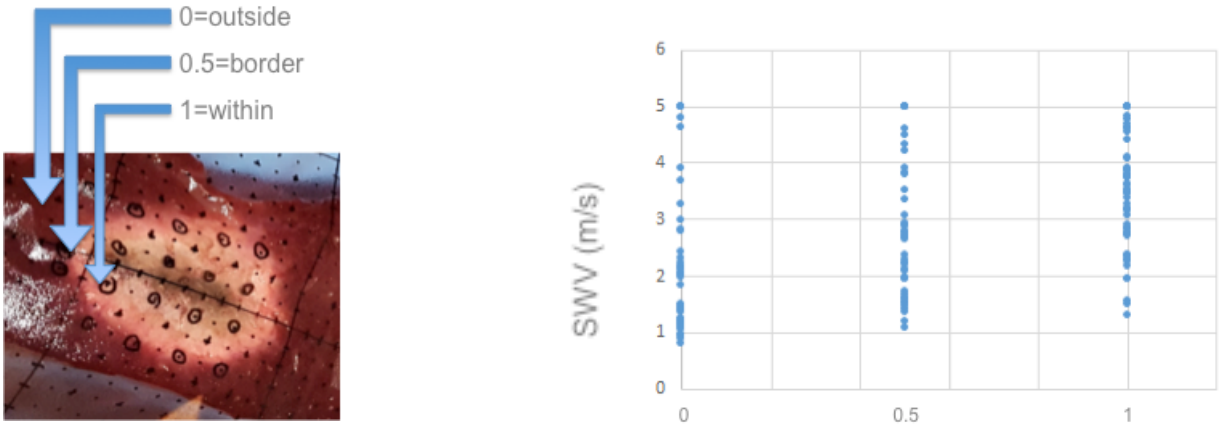

Fig. 11. SWV values measured in ROIs outside, at the border and within the ablated area are dispersed.

In order to explain these findings, we evaluated and represented graphically the SWV(± SD) measurement over time and demonstrated that during the ablation the values were constantly increasing until the Avg60 (3 m/s) is reached. After ablation interruption, SWV value - measured in the same ROI- gradually decreases, until reaching the baseline value in about 5 minutes time. (Fig.12)

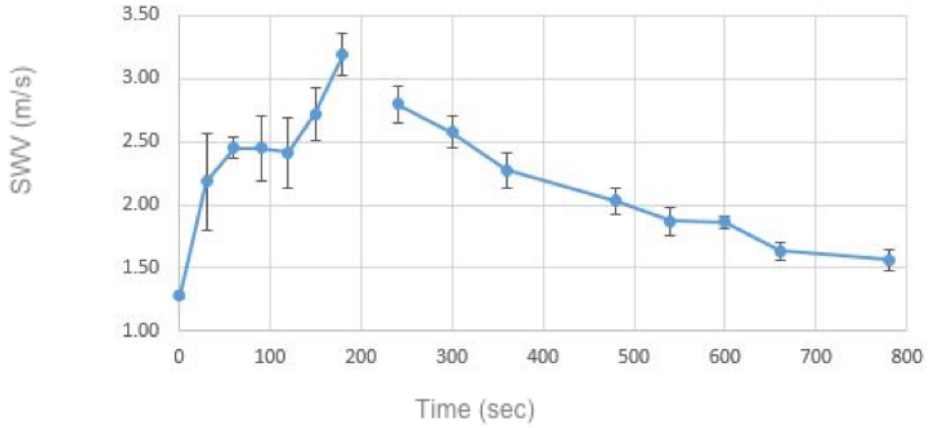

Fig 12. SWV(± SD) measurement over time: values were increasing until the threshold was reached. They decreased after ablation interruption reaching the baseline value in about 5 minutes.

These findings may have the following explanations: it is has been demonstrated that significant tissue contraction follows MW in ex-vivo experimental models [10, 11,12]. This contraction is greater at the peripheral portions of the ablation. It is therefore likely that the SWV measurements at the end of the ablation were performed in not ablated tissue that "moved" - following tissue contraction - where the ROI was originally placed. Therefore the time needed to move the ROI in different locations and to measure SWV could have made it impossible to capture the overcoming of the threshold within, at the border, and outside the ablation zone.

DISCUSSION

Quantitative estimation of tissue stiffness by means of US-elastography has been shown of major importance because tissue stiffness during tissue coagulation is directly linked to the thermal dose [7].

Liver tissue stiffness is reproducibly affected by temperature changes in conditions of controlled hyperthermia. Our experiments demonstrated that liver stiffness significantly changes after heating, and when a mean SWV of 3 m/s was reached the temperature was above 60°C. Moreover, these results illustrated the good ability of shear wave imaging to evaluate the heated region even in the case of a moderate temperature elevation (42-60°C). These results were partially confirmed in the second phase of the study, where the threshold of 3m/s had 89% accuracy in identifying necrosis at pathology. However the measurements of SWV within, at the border, within and outside the ablation were dispersed, demonstrating the insufficiency of the technique at the moment to monitor ablation.

The fundamental principle of thermal ablation monitoring using US-elastography lies in that heat-ablated tissue is stiffer than normal, untreated tissue. Heat-induced cell necrosis in fact results in the elevation of the elastic modulus of proteins and soft tissue, including Young's modulus and SWV. The Young modulus, which is defined by cellular and higher levels of structural organization of tissue, is greatly affected by pathological or physiological changes in tissue structure. The elasticity of tissues results primarily from changes in configurational entropy. In

thermal ablation, the entropy of protein is increased due to heat-induced denaturation, in which the native protein structure is transformed into a more random structure [13]. As it strongly affects the tissue structure, thermal necrosis of a tissue should result in a dramatic change of tissue SWV. Actually, few papers studied the thermal effects on the elastic properties of liver tissues. Sapin de Brosses et al. 2011 showed that the quantitative stiffness changes of heated in vitro tissue samples are strongly correlated with the thermal dose. However, these preliminary works did not focus on the possibility of taking advantage of the temperature dependence of SWV of tissues to provide quantitative estimates of temperature changes [3]. The SWV of liver tissues before heating (at room temperature) was in the range of data reported in the literature [14,15]. The most complete study was conducted by Wu *et al* (2001) who identified three patterns, in ex vivo bovine muscle: (1) a reversible decrease of the SWV with increasing temperature between 20°C and 60°C, (2) an irreversible increase around 60°C corresponding to the threshold of denaturation and (3) an increase of the SWV during cooling for tissues that underwent an irreversible thermal damage. The decrease of stiffness up to 60°C was previously explained by collagen unfolding and the increase of stiffness above 60°C was explained by collagen denaturation [5]. It is known that protein molecules begin to uncoil (undergo denaturation) at roughly 38°C, and begin to shorten at temperatures as low as 54°C. As the tissue coagulates, water in the cells is forced out. At 77°C, the cells have shrunk as much as they can and most of the water in the cells that can be released through tissue coagulation has occurred [12,13]. Kiss et al. 2009 previously observed

the thermal changes in the complex Young's modulus of ex vivo canine and porcine livers at respectively 70°C and 75°C, assessed by mechanical dynamic compression tests [16]. The contraction of tissue and fluid loss manifests itself as increase in the complex modulus. Our results demonstrated that liver stiffness increased above a temperature of about 63°C. The reason for this SWV steep increase has been identified as collagen fiber denaturation [17]. In most organs, proteins such as collagen fibers or elastin are responsible for the stiffness and the elastic properties of tissues. At around 60°C, collagen fibers are denatured. Hydrogen bonds maintaining the collagen helices are broken [18,19].

However, little attention was paid to stiffness changes at small temperature increases before the attainment of the necrosis threshold. In the moderate temperature elevation (42-60°C) ARFI methods are found to be quantitative and can be used as a technique for temperature estimation. In particular, we observed at the lower temperature range (42-55°C), tissue SWV decreases with increasing temperature and the change can be reversed when temperature decreases. As previously demonstrated, this pattern of tissue mechanical property change reflects heat-induced intrinsic structure changes in tissue [20]. We believe that tissue SWV change of the specimens in this region is due to reversible protein denaturation, which can be dominated by protein unfolding/refolding. It has been experimentally confirmed that the elastic properties of a muscle fiber are regulated by the molecular elasticity of specific proteins, and the major component of the protein elasticity are the unfolding/refolding reactions [17]. The elastic modulus of protein decreases with

unfolding, as in our case, of about -0.31 ± 0.07 m/s with respect to baseline at average temperature of 42°C. These tendencies are consistent with thermally induced proteins denaturation reported in Literature.

One of challenges to using US-based modulus imaging techniques in abdominal organs is that controllable displacements or deformations are difficult to be applied to the site being imaged. It is well understood that large errors among displacement estimates obtained from complex in vivo tissue motion may significantly hamper our efforts in obtaining accurate modulus images [14, 18]. To overcome this problem, we adopted a controllable and reproducible method to assess the elasticity of tissue during heating, achieved by the stability of our set-up. Since heating time has an impact on tissue mechanical property change, the heating rate has been kept constant throughout the controlled heating experiments in order to make all the results comparable. The reproducibility among experiments that we obtained enables us to quantify stiffness heterogeneity in the image and small stiffness changes under thermal constraints.

In the cool down we measured SWV values of 4.40 ± 0.41 m/s every 10°C until 50°C was reached, when non-numerical measurements were recorded in all evaluations, proving the irreversibility of changes in liver stiffness. Thus, irreversible cellular damage is obtained increasing the tissue temperature to 60°C [13].

Brosses et al. 2010 studied only three samples extracted from one bovine liver and 19 samples from 14 bovine muscles. Unlike our work, their SWV was almost constant up to 45°C and exponentially increased above 45°C. However, thermal

effects on stiffness were shown to be completely different between liver tissue and muscular tissue of bovines [6]. Therefore, at tissue level, there is currently no globally accepted thermo mechanical model that describes the changes of the SWV with temperature because of the lack of knowledge of the complex intra-tissue interactions [21,22].

If the results of the first phase were encouraging, in the second phase we experienced some unexpected events. A SWV of 3 m/s was confirmed to be an accurate threshold for identifying the region of coagulated tissue. However we found that after interrupting the ablation tissue properties continues to change, differently from the phase 1 experimental setup where the tissue was heated homogenously. We hypothesize that the coagulation induced abruptly by MW ablation was followed by shrinkage of the ablated tissue and changes in the surrounding non ablated tissue. Farina et al. demonstrated substantial shrinkage of 52-74% of initial tissue volume in a liver and muscle ex vivo animal model after MW ablation. The shrinkage was non-uniform over time and space, with observed asymmetry favouring the radial (23-43 % range) over the longitudinal (21-29%) direction. Algorithmic relationships for the shrinkage as a function of time were demonstrated. Additionally, CT imaging demonstrated initial expansion of the tissue volume, lasting in some cases up to 3 min during the MW ablation procedure, prior to the contraction phenomenon [12]. Similar results have been demonstrated by Weiss et al [11]. The correlation between shrinkage and dehydration was investigated by Brace at al, in an ex vivo experimental model. Besides confirming that after MW there is substantially superior

tissue shrinkage with respect to radiofrequency ablation (30-38% vs 15-30%), the Authors found a positive correlation between the percentage of water removed and relative contraction in liver. However, compared with RF, they found that MW created more dehydration at the inner position but less dehydration at the peripheral position [10]. These results might be partially explained by the hypothesis that water vapour driven from the inner position re-condensed and artificially increased water content in the middle and peripheral positions of MW ablations. Such an effect may be less likely with radiofrequency energy as the maximum temperature threshold is only 100°C [10, 23, 24]. The re-condensation of water in middle and peripheral portions of ablation zones, together with shrinkage of the inner portion, could represent the explanation why SWV values gradually came back to pre-ablation values after MW ablation interruptions. We were sampling in a different region due to shrinkage and it was likely that water content was increasing in that region.

Our study has some limitations. First, the experiments were conducted in ex-vivo liver tissue. Second the set-up was ideal, with homogeneous increase in the heating of the sample in the Phase 1 and extreme stability of the US probe/liver sample during measurements. These could make the results difficult to reproduce in in-vivo experiments. A further limitation to this study was the use of non-perfused ex vivo tissues. Further study will be needed to determine whether these findings are confirmed in a perfused or in vivo model. In vivo testing should also help determine whether the ablation zone rehydrates and expands after ablation. The study was also limited in its use of normal tissue. For example cirrhotic liver has a baseline SWV

higher than 2 m/s and this could cause interpretative difficulties when using pSWE during ablation. Tumours with different histology, may also behave differently during and after MW ablation according to their components (fat, fibrous tissue, etc.). These hypotheses need additional testing for verification.

Indeed, our work provides significant improvement in the description of thermal effects on liver tissues mechanical properties.

CONCLUSIONS

SWV is useful to monitor thermal changes in tissue in the setting of controlled hyperthermia. pSWE can provide an elasticity threshold predictive of the presence of coagulation necrosis during MW ablation in ex-vivo liver model. The complexity of ablation process in tissues, and possibly the shrinkage and re-hydration occurring after ablation, makes pSWE not able to reliably capture changes of stiffness within, at the border, and outside the ablation zone in this experimental model.

REFERENCES

1. Goldberg SN, Grassi CJ, Cardella JF et al. Image-guided tumor ablation: standardization of terminology and reporting criteria. Radiology. 2005 Jun; 235(3):728-39.
2. Zhou Z, Wu W, Wu S et al. A survey of ultrasound elastography approaches to percutaneous ablation monitoring. Proc Inst Mech Eng H. 2014 Oct; 228(10):1069-82.
3. Brosses ES, Pernot M, Tanter M. The link between tissue elasticity and thermal dose in vivo. Phys Med Biol. 2011 Dec 21; 56(24):7755-65.
4. Barr RG, Ferraioli G, Palmeri ML et al. Elastography Assessment of Liver Fibrosis: Society of Radiologists in Ultrasound Consensus Conference Statement. Radiology 2015 Sep; 276(3):845-61.
5. Wu T, Felmlee JP, Greenleaf JF et al. Assessment of thermal tissue ablation with MR elastography. Magn Reson Med. 2001 Jan;45(1):80-7.
6. Brosses ES, Gennisson JL, Pernot M et al. Temperature dependence of the shear modulus of soft tissues assessed by ultrasound. Phys Med Biol. 2010 Mar 21; 55(6):1701-18.
7. Mariani A, Kwiecienski W, Pernot M. Real time shear waves elastography monitoring of thermal ablation: in vivo evaluation in pig livers. J Surg Res. 2014 May 1; 188(1):37-43.

8. Ferraioli G, Tinelli C, Lissandrin R et al. Point shear wave elastography method for assessing liver stiffness. World J Gastroenterol. 2014 Apr 28; 20(16):4787-96.
9. Lee YJ. Shear Wave Elastography: a reliable and outperforming diagnostic tool for liver fibrosis assessment in chronic hepatitis. A literature review. Supersonic Imagine. The Theragnostic Company.
10. Brace CL, Diaz TA, Hinshaw JL et al. Tissue Contraction Caused by Radiofrequency and Microwave Ablation: A Laboratory Study in Liver and Lung. J Vasc Interv Radiol 2010; 21:1280–1286.
11. Weiss N, Goldberg SN, Nissenbaum Y, et al. Planar strain analysis of liver undergoing microwave thermal ablation using x-ray CT. Med Phys. 2015 Jan; 42(1):372-80.
12. Farina L, Weiss N, Nissenbaum Y, et al. Characterisation of tissue shrinkage during microwave thermal ablation. Int J Hyperthermia. 2014 Nov; 30(7):419-28.
13. Arnal B, Pernot M, Tanter M. Monitoring of thermal therapy based on shear modulus changes: II. Shear wave imaging of thermal lesions. IEEE Trans Ultrason Ferroelectr Freq Control. 2011 Aug; 58(8):1603-11.
14. Fahey BJ, Nelson RC, Hsu SJ et al. In vivo guidance and assessment of liver radio-frequency ablation with acoustic radiation force elastography. Ultrasound Med Biol. 2008 Oct; 34(10):1590-603.
15. Fahey BJ, Hsu SJ, Wolf PD et al. Liver ablation guidance with acoustic radiation force impulse imaging: challenges and opportunities. Phys Med Biol. 2006 August 7; 51(15): 3785–3808.

16. Kiss MZ, Daniels MJ, Varghese T. Investigation of temperature-dependent viscoelastic properties of thermal lesions in ex vivo animal liver tissue. J Biomech. 2009 May; 42(8):959-66.
17. Lepetit J. A theoretical approach of the relationships between collagen content, collagen cross-links and meat tenderness. Meat Sci. 2007 May;76(1):147-59.
18. Jiang J, Varghese T, Brace TL et al. Young's Modulus Reconstruction for Radio-Frequency Ablation Electrode-Induced Displacement Fields: A Feasibility Study. IEEE Trans Med Imaging. 2009 Aug; 28(8):1325-34.
19. Zhu Y, Hall TJ and Jiang J. A finite-element approach for Young's modulus reconstruction. IEEE Trans. Med. Imag. 2003 Jul; 22(7):890–901.
20. Rossmann C, Garrett-Mayer E, Rattay F et al. Dynamics of tissue shrinkage during ablative temperature exposures. Physiol Meas. 2014 Jan;35(1):55-67.
21. Sugimoto K, Oshiro H, Ogawa S et al. Radiologic-pathologic correlation of three-dimensional shear-wave elastographic findings in assessing the liver ablation volume after radiofrequency ablation. World J Gastroenterol. 2014 Sep; 20(33):11850-5.
22. Dewall RJ, Varghese T and Brace TL. Visualizing ex vivo radiofrequency and microwave ablation zones using electrode vibration elastography. Med Phys. 2012 Nov; 39(11):6692-700.
23. Yang D, Converse MC, Mahvi DM, Webster JG. Measurement and analysis of tissue temperature during microwave liver ablation. IEEE Trans Biomed Eng 2007; 54:150 –155.

24. Yang D, Converse MC, Mahvi DM, Webster JG. Expanding the bioheat equation to include tissue internal water evaporation during heating. IEEE Trans Biomed Eng 2007; 54:1382–1388.